Microstructural Polymorphism in Bovine Brain Galactocerebroside and Its Two Major Subfractions†

Douglas D. Archibald‡

Department of Chemistry, University of Washington, Seattle, Washington 98195

Paul Yager*

Molecular Bioengineering Program, Center for Bioengineering, FL-20, University of Washington, Seattle, Washington 98195

Received December 2, 1991; Revised Manuscript Received June 1, 1992

ABSTRACT: Aqueous suspensions of either brain galactocerebrosides or its subfraction consisting of α-hydroxyacyl galactocerebrosides are mainly composed of vesicles or granular lipid with occasional multilamellar sheets. In aqueous media the other subfraction consisting of non-hydroxyacyl galactocerebrosides forms some helical structures, but most of the lipid remains as granules or vesicles. It is demonstrated that thermal cycling of non-hydroxyacyl galactocerebrosides in polar nonaqueous solvents can greatly enhance the degree of conversion to helical ribbons about 100 nm in diameter. These structures appear to be a stable dehydrated crystalline form of this lipid and are morphologically similar to helical microstructures produced by a few synthetic lipids. On the other hand, similar treatment of unfractionated bovine brain cerebroside and its α-hydroxy fatty acyl subfraction quantitatively produces straight needles that appear to be cochleate cylinders. While their dimensions depend on formation conditions, a typical suspension has uniform particles with diameters close to 100 nm and lengths variable from one to a few hundred micrometers. This is the first report demonstrating the quantitative formation of crystalline high axial ratio microstructures from complex mixtures of natural lipids. The different microstructures formed by the two components appear related to the various forms of lipid deposits occurring in lipid storage diseases. The similarity of these "synthetic" microstructures to biological structures in which they are found (such as myelin and intestinal brush border microvilli) strengthens the possibility that galactocerebrosides have a role in stabilizing cylindrical biological structures.

Recently there has been significant interest in regular high axial ratio microstructures that spontaneously self-organize. The research has focused on synthetic or semisynthetic two-chain amphiphiles that, when dispersed in aqueous media, form bilayer rods, tubules, or helices rather than liposomes (Yager et al., 1992). Technological interest in high axial ratio lipid microstructures was sparked by experiments on several synthetic systems that form hollow bilayer tubules or helices; the lipids include lecithins containing diacetylene moieties in both acyl chains (Georger et al., 1987; Yager & Schoen, 1984; Yager et al., 1985), surfactants in which a glutamic or aspartic acid residue is substituted with two alkyl chains and an alkylammonium chain (Nakashima et al., 1984, 1985), *N*-octylaldonamide single-chain surfactants (Fuhrhop et al., 1987, 1988), amphiphiles containing a headgroup of oligoglutamic acid (Yamada et al., 1984), and perhaps also mixtures of 1,2-dimyristoyl-*sn*-glycero-3-phosphocholine and its chemical degradation products (Servuss, 1988).

In all these tubular, helical, and rod-like microstructures, the bilayer is believed to be in a crystalline state, perhaps one with extremely long range helical order (Blechner et al., 1990; Rhodes et al., 1987, 1988). While several theoretical approaches toward predicting the structure of tubules and helices have been made (Chappell & Yager, 1991a,b,c; de Gennes 1987; Helfrich, 1986; Helfrich & Prost, 1988), none of these models allows a detailed specific prediction as to the nature of the molecular packing in the tubule or helix bilayer, so there is no a priori method for either picking or designing a lipid that might form tubular or helical microstructures.

Promising applications may exist for high axial ratio lipid microstructures (Rudolph et al., 1988; Schnur et al., 1987), and therefore there is interest in finding novel methods of preparing microstructures, as well as microstructures with new chemical properties. This work examines conditions of formation and the properties of microstructures formed by biologically derived cerebrosides. Cerebrosides are involved in a number of high axial ratio biological structures such as myelin, and moreover it forms the anisotropic deposit in the lipid storage diseases globoid-cell leukodystrophy (GLD) (Suzuki & Suzuki, 1989) and Gaucher's disease (Lee et al., 1973). The process of formation of various kinds of GLD deposits is not completely understood.

The cerebroside that forms the GLD deposits is referred to as galactosylceramide or galactocerebroside (Gal-Cer). Cerebroside itself is a complex class of lipids characterized by a sphingosine backbone with an amide-linked long-chain fatty acid and a single glycosidic-linked sugar residue (see Figure 1). Adult human brain cerebrosides are almost exclusively galactose-containing with more than 95% C_{18}-sphingosine [D(+)-*erythro*-1,3-dihydroxy-2-amino-4-*trans*-octadecene]. The remainder is mostly C_{18}-dihydrosphingosine and a much smaller amount of C_{16}-sphingosine. The amide-linked fatty acids are generally long (C_{20}–C_{26}) and not polyunsaturated, and approximately two-thirds are α-hydroxylated. For bovine brain, the acyl composition of the extract has been reported (Johnston & Chapman, 1988). Compared

† This work was supported by National Science Foundation Grant CTS-8815027 (P.Y.).

* To whom correspondence should be addressed.

‡ Current address: School of Chemistry, University of Bath, Claverton Down, Bath BA2 7AY, England.

0006-2960/92/0431-9045$03.00/0

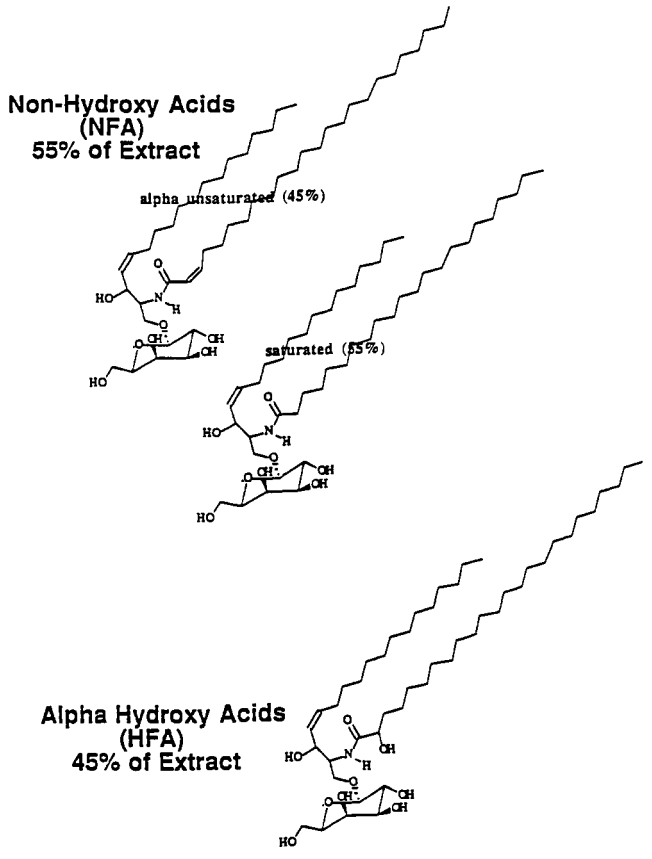

FIGURE 1: Molecular structures and composition of bovine brain cerebroside.

to the non-hydroxy cerebrosides (NFA-Gal-Cer), α-hydroxy cerebrosides (HFA-Gal-Cer) have a greater proportion of longer chains (Suzuki & Suzuki, 1989).

Two groups have reported negative stain electron microscopy studies of lipid microstructures containing purified Gal-Cer. McCabe and Green (1977) noted the formation of what appeared to be 30 × 200 nm cylindrical liposomes from a sonicated dispersion of brain cerebrosides and cholesterol. Curatolo and Neuringer (1986) noted the formation of multilamellar tubules from dispersions of brain cerebrosides alone or when mixed with 1-palmitoyl-2-oleoyl-phosphatidylcholine (POPC). Their preparation technique involved vortexing aqueous suspension of a lyophilized powder. They also examined semisynthetic C16:0-NFA-Gal-Cer. This lipid formed 100-nm diameter tubules alone or when mixed with POPC or cholesterol. No high axial ratio microstructures have been reported for HFA-Gal-Cer.

This paper reports successful quantitative conversion of these natural biological lipids into *two distinct classes* of regular high axial ratio lipid microstructures. When thermal cycling of the lipids is performed in the presence of high concentrations of certain glycols, NFA-Gal-Cer and Gal-Cer produce structures resembling the helices found for diacetylenic phosphatidylcholines (Georger et al., 1987). HFA-Gal-Cer under the same conditions produces structures that appear needle-like by optical microscopy and bear a strong resemblance to tubular diacetylene phospholipid microstructures (tubules) (Yager & Schoen, 1984; Yager et al., 1985) and to cochleate cylinders (Papahadjopoulos et al., 1975). The HFA-Gal-Cer microstructures bear a strong resemblance to myelin; while a similar relationship between cerebroside microstructure and natural structures was pointed out by Curatolo and Neuringer (1986), their results differ substantially from ours.

EXPERIMENTAL PROCEDURES

Materials. Lyophilized bovine brain cerebroside was obtained from Avanti Polar Lipids (Pelham, AL), while lyophilized bovine brain NFA-Gal-Cer and HFA-Gal-Cer were obtained from Sigma Chemical Co. (St. Louis, MO). All lipids were nominally of better than 99% purity. 1,2-Ethanediol (ethylene glycol) was reagent grade (nominally 100%; manufacturer's analysis, 0.002% CH_3COOH, 0.0009% residue after ignition; J. T. Baker, Phillipsburg, NJ). Water was deionized and doubly distilled. Other solvents that were used are identified as follows: 1,2-propanediol (propylene glycol, Gold label, racemic, nominally 99+%; Aldrich Chemical Co., Milwaukee, WI); glycerol (reagent grade, manufacturer's analysis, 100.2%; J. T. Baker); absolute methanol (reagent grade, nominally 100.0%; J. T. Baker); 95% ethanol (Midwest Grain Co., Pekin, IL); *n*-propanol (reagent grade; Alfa, Danvers, MA); pyridine (chromatography grade, nominally 99.9%; EM Science, Cherry Hill, NJ); and dimethyl sulfoxide (Ultrapure grade, nominally 99+%; Alfa). Salts and polar solutes that were used include D-galactose (purified grade, Sigma), NaCl (manufacturer's analysis, 99.3%, <0.001% Ca^{2+} and Mg^{2+}; J. T. Baker); $CaCl_2$ (reagent grade; J. T. Baker), HCl (reagent grade; J. T. Baker) and NaOH (reagent grade pellets, nominally 98.9%; J. T. Baker).

Thin-layer chromatographic analysis was performed on 200–300-μg specimens of the microstructure preparation as well as the lipid as obtained from the manufacturers. Microstructure preparations were first concentrated by centrifuging/decanting/drying at room temperature. All lipids were spotted on silica gel plates (J. T. Baker, Si250) from chloroform/methanol (2:1). Spotted on the same plate were 40-μg loadings of potential hydrolysis products including psychosine, 2-hydroxyhexacosanoic acid, tetracosanoic acid, D-sphingosine, and bovine brain ceramide (all nominally >99% purity and used as obtained from Sigma). The developing solution consisted of chloroform/acetone/methanol/acetic acid/water (65:35:11:4:1.5). Spots were indicated by first observing refractive index variations after spraying with $K_2Cr_2O_7$-saturated 50% sulfuric acid and then by charring. No evidence of cerebroside impurities or breakdown products was detected in these lipid microstructure preparations.

Preparation of Lipid Microstructures. Thermal cycling in nonaqueous solvent was used to overcome the poor dispersability of aqueous cerebrosides. Suspensions of powdered lipid at 10 mg/mL in 95% 1,2-ethanediol (ethylene glycol) (w/w) or other solvents were typically prepared by incubation at 99 °C for 15 min followed by hand swirling for 2 min with continued incubation. The sample vial was then sonicated for 10 min in a 50 °C water bath (model G1128P1G, output 80 kilocycles, 80 W, Laboratory Supplies Co., Hicksville, NY) for 10 min. Although not essential, sonication proved more effective than hand mixing. Incubation, hand swirling, and sonication procedures were generally repeated three times until a uniform suspension was obtained. The last steps in sample preparation were a 15-min incubation without stirring followed by slow cooling to 25 °C (at ≤0.6 °C/min).

The suspending medium used in the thermal cycling procedure was varied in order to find optimal preparation conditions and to explore the mechanisms of formation and stabilization. Suspending solvents included 1,2-ethanediol, 1,2-propanediol, glycerol, dimethyl sulfoxide, methanol, ethanol, or *n*-propanol, each mixed with various portions of water. Solutions of 0.25 M NaCl, $CaCl_2$, or D-galactose in 95% 1,2-ethanediol/5% water were used to determine whether ions or polar solutes would perturb microstructure formation. To

examine the effect of acid or base, 1,2-ethanediol was mixed with 10% aqueous 0.01 or 1 M HCl or NaOH.

Preparation of microstructures by solvent precipitation was performed by dissolving the lipid in room temperature pyridine and then adding water or a solvent composed of 90% 1,2-ethanediol/10% water (w/w) with gentle mixing for a few seconds. Samples were allowed to precipitate overnight or longer. The final lipid concentration was typically 1 mg/mL. Pyridine concentrations typically ranged from 50% to 95% (v/v), but some samples were prepared at pyridine concentrations below 5%.

Instrumental Methods. Differential scanning calorimetry (DSC) was performed with a Seiko DSC 100 (Seiko Instruments USA, Inc., Torrance, CA) with the use of 70-μL hermetically sealed silver pans at a scanning rate of ±0.2 °C/min. For DSC experiments, cerebroside microstructures were prepared in the silver pans by incubating the lipids in appropriate solvents at 95 °C with sonication. Samples were then cooled slowly to room temperature before beginning scans in the calorimeter. Phase contrast optical micrographs were taken using a Zeiss ICM 405 (Carl Zeiss, Inc., Thornwood, NY) with 40× (NA 0.75), 63× (NA 1.4, oil), or 100× (NA 1.25, oil) phase contrast lenses. Sample heating while viewing with an optical microscope was performed by use of a small diameter nichrome heating wire sandwiched with the sample between two cover glasses. Heat output was controlled with a rheostat. No attempt was made to calibrate structural transitions to a particular sample temperature.

Scanning electron microscopy (SEM) was performed with a Hitachi S-800 field emission microscope on loan from the manufacturer (Tokyo, Japan). Samples for SEM were deposited directly onto an aluminum stub, air-dried, and imaged without coating at low accelerating voltages. Both transmission electron microscopy (TEM) and freeze-fracture electron microscopy employed a JEOL 1200 (Peabody, MA) with an 80-kV accelerating potential. For TEM, samples in water were deposited directly onto carbon/Formvar-coated copper grids. The procedure for samples in 95% 1,2-ethanediol was similar, except that the sample was first diluted with water approximately 1:1000.

For preparation of freeze-fracture replicas, samples were quickly frozen by immersion of the gold sample holders into a LN_2 cooled slush of Freon. The samples were cooled to −115 °C during fracturing under a vacuum of 4–9 × 10^{-6} torr in a Balzers Freeze-Etch device (Hudson, NH). The knife blade was cooled to less than −160 °C. An 18-Å coating of Pt–C from an electron sputtering device was applied at an angle of 45°. Several hundred angstroms of carbon from an electrode was then applied normal to the surface fracture. The sample was melted in water and cleaned by transferring it in several steps through pyridine and back to water. The cleaned replica pieces were transferred to Formvar-coated copper grids. Replicas were dried at room temperature before viewing by TEM. Micrographs shown were printed directly from film from the microscope (using "light shadows") except as noted.

Low-angle X-ray scattering (model 3488K diffractometer, Picker X-ray Corp., Waite Manufacturing Division, Inc., Cleveland, OH) was performed on concentrated suspensions of HFA-Gal-Cer deposited on glass slides. Molecular modeling was performed on a Macintosh IIci microcomputer (Apple Computers, Inc., Cupertino, CA) using a molecular modeling program (Chem3DPlus, Cambridge Scientific Computing, Inc., Cambridge, MA) that included MM2 energy minimization routines.

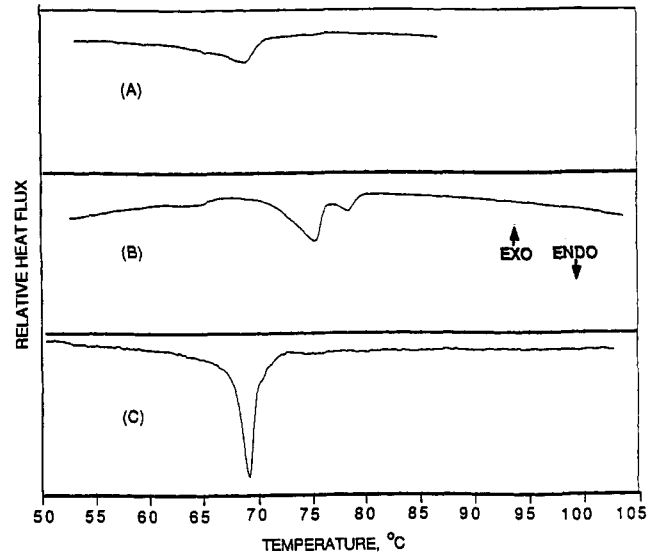

FIGURE 2: DSC of Gal-Cer microstructure preparations in water: (A) Gal-Cer; (B) NFA-Gal-Cer; and (C) HFA-Gal-Cer.

RESULTS

Many different protocols were explored for quantitative conversion of Gal-Cer and its two subfractions into high axial ratio microstructures. Initial attempts using simple thermal cycling in water, which had been successful for diacetylenic PCs, for example (Burke et al., 1988; Yager et al., 1988; Yager & Schoen, 1984), failed. "Solvent precipitation" (Georger et al., 1987), which is simply crystallization from small micelles or individual molecules in solution, is an attractive method for forming lipid microstructures because it reduces chemical breakdown and affords better control of microstructure morphology than thermal cycling. The insolubility of Gal-Cer in most alcohols initially prevented us from using simple precipitation from isotropic solution. The protocol that eventually proved successful was a combination of both approaches in which thermal cycling of the lipid was carried out in extremely high concentrations of glycols, particularly 1,2-ethanediol and 1,2-propanediol. These solvents greatly shifted the phase-transition temperatures of Gal-Cer and its subfractions. Thermal effects of 1,2-ethanediol and 1,2-propanediol were mirrored by dramatic changes in the microstructure suspensions.

Differential Scanning Calorimetry. First heating DSC scans of lipids in water and 95% 1,2-ethanediol are displayed in Figures 2 and 3, respectively. In all cases, the temperature of the gel-to-liquid-crystalline transitions were significantly increased in glycol–water mixtures over those measured in pure water. As expected, the melting transitions of the mixture Gal-Cer tend to be broader than those of its subfractions, but there are no distinct peaks indicating even partial phase separation of its two components. Suspension of NFA-Gal-Cer in 95% 1,2-ethanediol greatly reduces the thermogram complexity compared to that of the suspension in water. Both Gal-Cer and HFA-Gal-Cer in 95% 1,2-ethanediol have two distinct heating endotherms. The cooling transitions subsequent to these heating transitions are even more complex (Archibald, 1990), reflecting the well-known metastability of the cerebroside–water system (Bunow, 1979; Curatolo, 1982, 1985; Curatolo & Jungalwala, 1985).

In 95% 1,2-propanediol, the main endotherms all occur at temperatures that are higher than those observed in water but lower than those observed in 95% 1,2-ethanediol. The transitions of Gal-Cer and HFA-Gal-Cer in 95% 1,2-pro-

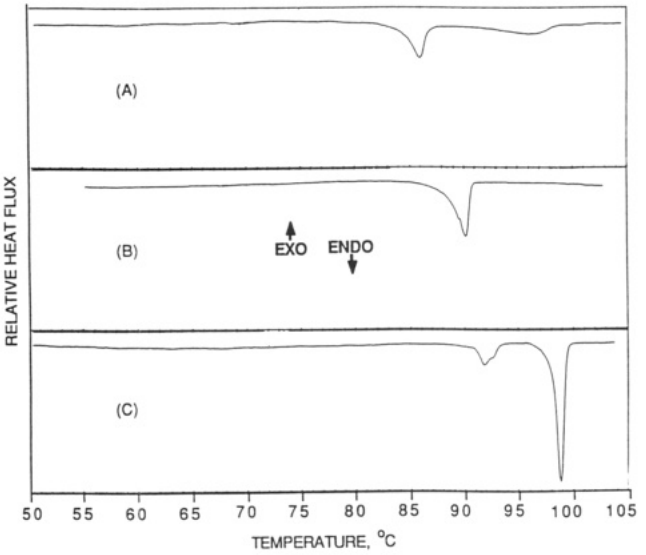

FIGURE 3: DSC of Gal-Cer microstructure preparations in 95% 1,2-ethanediol: (A) Gal-Cer; (B) NFA-Gal-Cer; and (C) HFA-Gal-Cer.

Table I: Solvent Dependence of Melting Transition Temperatures of Cerebrosides[a]

	solvent system		
cerebroside	H_2O	95% 1,2-propanediol in water	95% 1,2-ethanediol in water
Gal-Cer	68.8	84.5	86.0, 96.2
NFA-Gal-Cer	64.0, **75.3**, 78.3	73.3, 81.6, **87.1**	90.1
HFA-Gal-Cer	68.9	87.2	92.0, **98.9**

[a] In cases in which there are multiple endotherms, the largest endotherms is shown in boldface. The two endotherms of Gal-Cer in 1,2-ethanediol are of similar enthalpy, but the lower endotherm is substantially sharper.

panediol have long sloping pretransitions and lack the second transition peaks that were observed in the corresponding samples in 95% 1,2-ethanediol. The thermal behavior of NFA-Gal-Cer in 95% 1,2-propanediol appears much more complex than in 95% 1,2-ethanediol. A large degree of hysteresis in the cooling transitions of HFA-Gal-Cer and Gal-Cer, similar to that found in 95% 1,2-ethanediol, is observed when these lipids are suspended in 95% 1,2-propanediol. Likewise, poor repeatability of peak positions was found on subsequent cooling cycles without remixing. The temperatures of the heating endotherms of the three lipids in water and both glycols are listed in Table I.

Aqueous Dispersions of Cerebrosides. The difficulty of dispersing Gal-Cer in water has been noted in the literature (McCabe & Green, 1977), and this property is shared by HFA-Gal-Cer and NFA-Gal-Cer. TEM and optical microscopy of NFA-Gal-Cer dispersed in water reveal this sample to be a precipitate composed mostly of a coagulated mass of multilamellar vesicles. However, occasional elongated ribbons are also present, and many of these are twisted (see Figure 4). Water preparations of Gal-Cer and HFA-Gal-Cer are predominantly a dense coagulation of lipid with irregular lamellar structures.

Solvents Promote Conversion of NFA-Gal-Cer Dispersions into a Gel of Twisted Ribbons and Helices. After thermal cycling in 95% 1,2-ethanediol, preparations of NFA-Gal-Cer form a semitransparent viscoelastic gel. Optical microscopy indicates complete conversion of NFA-Cer to an interwoven network, of flexible fibrils of indeterminate length (see Figure

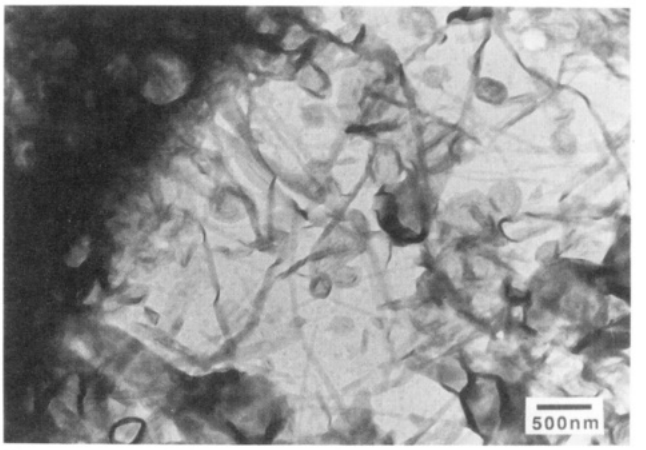

FIGURE 4: Transmission electron micrograph of NFA-Gal-Cer prepared by thermal/mechanical cycling in water.

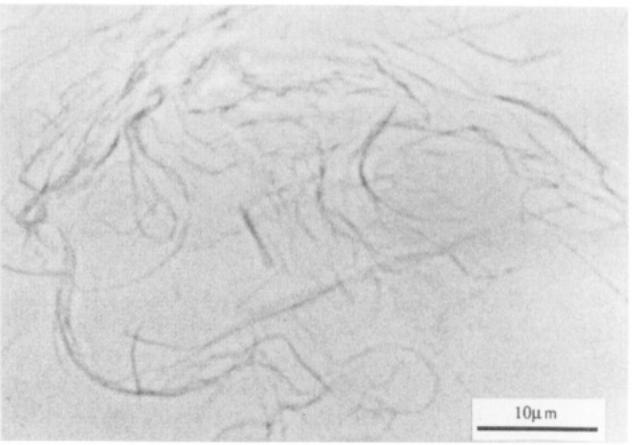

FIGURE 5: Optical micrograph of NFA-Gal-Cer prepared by thermal/mechanical cycling in 95% 1,2-ethanediol.

5). The filamentous NFA-Gal-Cer gel forms in 95% 1,2-ethanediol even during rapid (>10 °C/min) cooling from above the order–disorder transition, as well as in moderately acidified or basicified 90% 1,2-ethanediol. High acid concentration inhibits gel formation. Similar gels were produced by thermal cycling in other water-miscible solvents including 95% 1,2-propanediol and 50% ethanol.

Fibril network gels are also produced by precipitation of NFA-Gal-Cer from pyridine solution with either 90% 1,2-ethanediol or water (see Figure 6). Optical microscopic examination of the precipitation process reveals that pyridine/water solutions supersaturated with NFA-Gal-Cer precipitate first as vesicle-like structures that convert to fibrils within a few minutes (data not shown).

The predominant microstructure of NFA-Gal-Cer prepared by thermal cycling in 95% 1,2-ethanediol was a helical ribbon (see Figure 7). The helices observed were often several microns in length, but longer helices generally were entwined with others, making length measurement difficult. Different electron densities indicate that at least a portion if not all of the structures are composed of multilayers. Some of the microstructures appear as flat ribbons, and in other microstructures the helical wraps join to form cylinders like those found in diacetylenic phosphatidylcholines (see Figure 7). Cylinder diameters varied over the range from 50 to 105 nm (sample size of seven). The width of the ribbons varied between 39 and 84 nm (sample size of six). The gradient angle of the open helices varied between 51° and 75° while the helical pitch varied between 270 and 605 nm (sample size of seven not including cylinders, which generally have a smaller pitch).

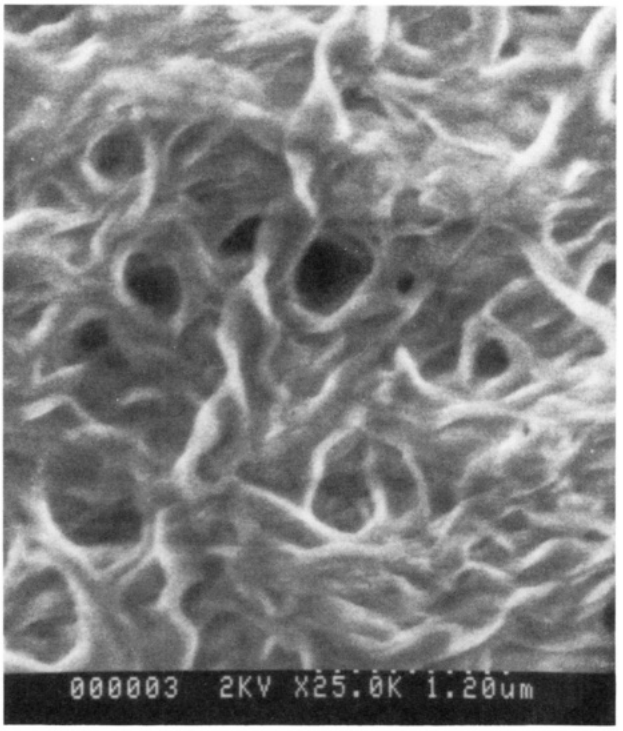

FIGURE 6: Scanning electron micrograph of NFA-Gal-Cer prepared by precipitation from pyridine with 20% water.

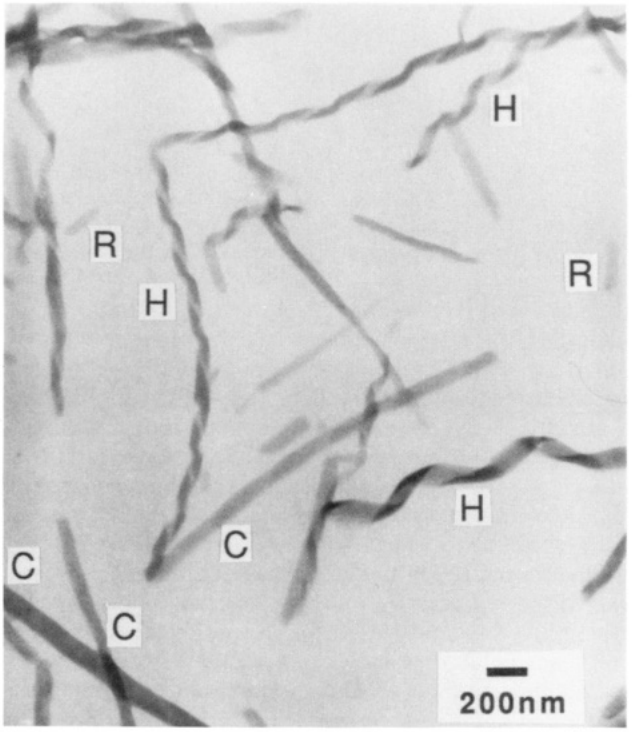

FIGURE 7: Transmission electron micrograph of NFA-Gal-Cer prepared by thermal/mechanical cycling in 95% 1,2-ethanediol: H, helical ribbons; R, flat ribbons; and C, cylinder composed of helical ribbons.

The measurements of gradient angle and pitch are probably perturbed by the flattening that occurs during sample preparation. The ends of the helices (diameter approximately 0.5 μm) appear to be a ribbon with rounded edges. Cylinder ends appear blunt.

Some of the open helices observed by electron microscopy may be created as an artifact of sample preparation. Freeze-fracture replicas of the same samples produced mainly helically wrapped filled cylinders. The ends tend to break irregularly,

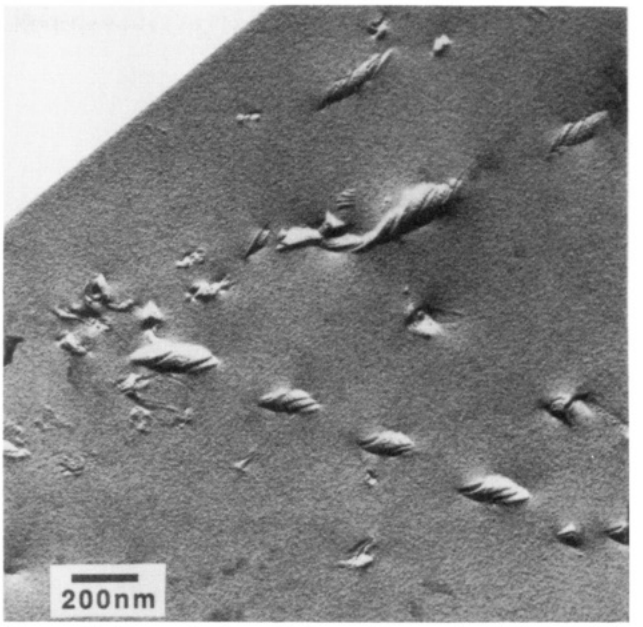

FIGURE 8: Freeze-fracture electron micrograph of NFA-Gal-Cer prepared by thermal/mechanical cycling in 95% 1,2-ethanediol.

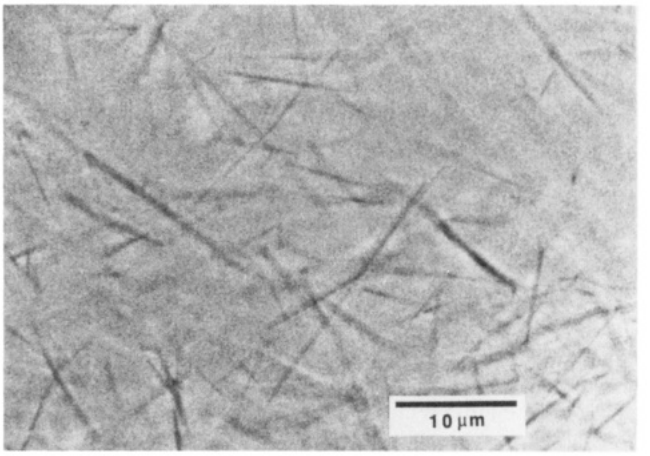

FIGURE 9: Optical micrograph of Gal-Cer prepared by thermal/mechanical cycling in 95% 1,2-ethanediol.

revealing separate inner lamellae that are not perfectly concentric. Typical closed cylinders are 85 ± 10 nm in diameter (mean ± SD of nine structures), with a helix gradient angle of ~60°, a pitch of about 275 nm, and a lumen diameter of less than 25 nm. Figure 8 shows two multilayered wrapped helices—another form that is present. In replicas of both kinds of structures, the individual wraps correspond to a single bilayer thickness. In some of the cylinders and helices the lamellae have regular striations with periodicities on the order of 100 Å; these run parallel with the helix edge, occasionally separated by channels so deep that the walls appear to be composed of individual fibrils.

Solvents Promote Conversion of HFA-Gal-Cer and Gal-Cer into Needles. The behavior of both HFA-Gal-Cer and Gal-Cer is quite different from that of the NFA fraction. When prepared in 90% or 95% 1,2-ethanediol, preparations of HFA-Gal-Cer and Gal-Cer form a cloudy suspension. Phase contrast optical microscopy indicates complete conversion of HFA-Gal-Cer and Gal-Cer to thick mats of rigid needles, typically in the range of 5–30 μm in length (see Figure 9). Once HFA-Gal-Cer needles are formed, they remain intact for an indefinite period in glycol solvents and survive desolvation under vacuum. When resuspended in water, some delamination of the needles is observed over a period of weeks.

HFA-Gal-Cer suspended in 95% 1,2-propanediol appears to be in a state intermediate between that in 95% 1,2-ethanediol and that in water. The lipid undergoes partial conversion to needles more irregular in diameter and length than those formed in 95% 1,2-ethanediol. Some of the needles have diameters exceeding 1.5 μm, and much of the lipid is in granular or multilamellar form. Larger needles show strong and often uniform birefringence when viewed under cross-polarization. Occasionally a thick sheet appears partially rolled up at one or two sides to form a needle or needle pair.

High concentrations of glycerol may also be suitable for partial needle formation. However, methanol, ethanol, *n*-propanol, and DMSO suspensions were devoid of large needles when cycled through conditions that produced needles quantitatively in 1,2-ethanediol. Samples prepared in high concentrations of these solvents occasionally had radially projecting dense fine fibrils emanating from granular lipid. Unlike the large cylinders produced in 95% 1,2-ethanediol, the diameters of these fibrils could not be resolved by optical microscopy.

Needles also form in strongly basic or weakly acidic 90% 1,2-ethanediol. Strongly acidic 1,2-ethanediol solutions inhibit formation, possibly because of acid-catalyzed hydrolysis of the amide or glycoside linkages of HFA-Gal-Cer. Pure ceramide or psychosine (products of hydrolytic cleavage of the galactosyl or acyl moiety, respectively) did not form needles by thermal/mechanical cycling in water or 90% 1,2-ethanediol.

HFA-Gel-Cer needles form readily in 90–100% 1,2-ethanediol. In lower concentrations of glycol in water, the lipid converts to small granular or lamellar particles. At very low 1,2-ethanediol concentrations, large vesicles and lamellar sheets are observed. If 95% 1,2-ethanediol containing 0.25 M Na^+ or Ca^{2+} is used as the suspending solvent, the needles still form quantitatively but appear larger and more irregular than those without the solutes. This change is even more pronounced when HFA-Gal-Cer needles were prepared in 0.25 M D-galactose-containing 95% 1,2-ethanediol. Part of the needles appeared as much larger diameter tapered rods, often with shorter rods attached in whorls. These larger irregular needles appear related to those prepared from Gal-Cer or HFA-Gal-Cer in 100% 1,2-ethanediol.

Optical microscopy indicated that heating destroyed previously formed mats of HFA-Gal-Cer needles only if the temperature was maintained above the melting temperature of the lipid in the solvent used (99 °C in 95% 1,2-ethanediol). Melting of mats of needles occurred rapidly, and the resulting globular mass often greatly expanded its volume. For isolated needles, melting can occur at several points along a needle, eventually converting the lipid to a globular mass that did not revert to needle form on cooling. Temperature control is important; fast cooling rates (>10 °C/min) can prevent needle formation or at least change the dimensions of the structures that are formed. Needle preparations slowly cycled through T_m on microscopy slides (without mechanical agitation) also were not found to revert to the needle form.

No needles were obtained from Gal-Cer under conditions that produced HFA-Gal-Cer needles in 95% 1,2-propanediol. However, there was no extensive attempt to optimize preparation parameters such as the mixing or incubation temperature and the percentage of 1,2-propanediol in the solvent.

An effort was made to prepare cerebroside needles by precipitation from solutions in organic solvents. Pyridine was the only solvent tried that was found to dissolve appreciable amounts of cerebrosides and to be miscible with water.

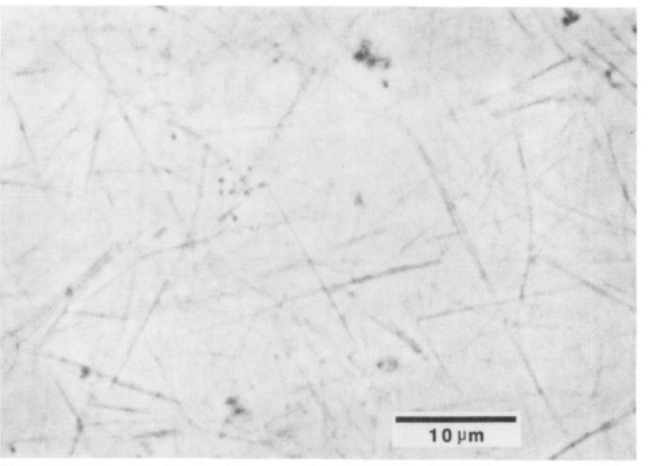

FIGURE 10: Optical micrograph of HFA-Gal-Cer prepared by precipitation from pyridine with 50% of a solution of 90% 1,2-ethanediol.

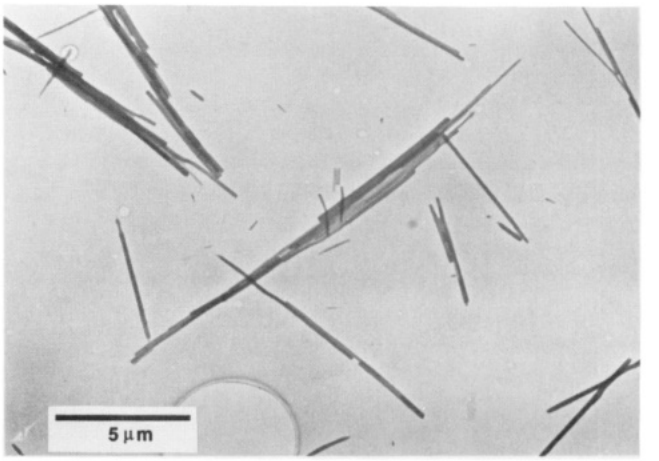

FIGURE 11: Transmission electron micrograph of HFA-Gal-Cer prepared by thermal/mechanical cycling in 95% 1,2-ethanediol.

Precipitation of HFA-Gal-Cer from pyridine with 90% 1,2-ethanediol/10% water sometimes resulted in partial conversion to long needles. These needles were generally of smaller diameters than those produced by thermal cycling in 95% 1,2-ethanediol. At high concentrations of pyridine, the lipid structure that was formed appeared similar to that of HFA-Gal-Cer prepared by thermal cycling in DMSO or monohydroxy alcohols. Intermediate concentrations showed partial needle formation (See Figure 10). A sample prepared at low pyridine concentration produced coagulations of short very small diameter fibrils, but no large needles. Water precipitation at intermediate pyridine concentration produces some small diameter flexible high axial ratio structures that are less regular than those seen in 1,2-ethanediol precipitation.

HFA-Gal-Cer needle length characterization is difficult because aggregation makes representative sampling difficult either by TEM or optical microscopy. The relatively large variability in the lengths is evident from a sampling of the needles in the transmission electron micrograph of Figure 11 (3.4 ± 1.9 μm, mean ± SD of 10 structures, rel SD of 55%). It is likely that many of these result from breakage of longer needles. While the distribution of lengths was much narrower in many samples, the mean length varied greatly among different sample preparations; some individual needles exceeding 300 μm were observed.

The diameters of the HFA-Gal-Cer needles produced by thermal cycling in 1,2-ethanediol microstructures vary greatly. Diameters can be much larger than any previously reported

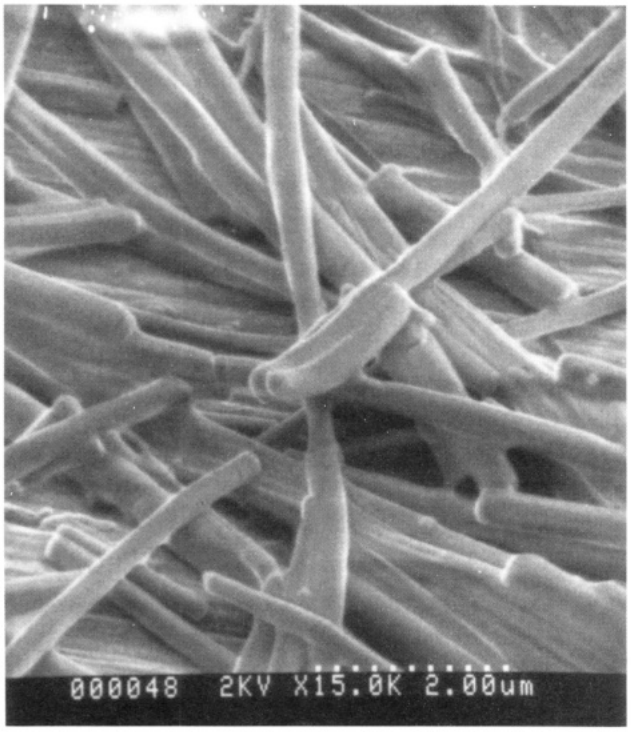

FIGURE 12: Scanning electron micrograph of HFA-Gal-Cer prepared by thermal/mechanical cycling in 95% 1,2-ethanediol.

for cerebroside suspensions [such as those seen by Curatolo and Neuringer (1986)], although some needle diameters below 70 nm were seen by transmission EM. TEM tends to favor sampling of the shorter, smaller diameter needles that do not clump together, so freeze-fracture EM or scanning EM data are more representative. One cluster of needles imaged by freeze-fracture EM yielded diameters of 141 ± 44 nm (mean ± SD of 20; rel SD = 31%), where the minimum was 100 nm and the maximum was 200 nm. Scanning electron microscopy (see Figure 12) of a cluster in a different sample yielded 327 ± 79 nm (mean ± SD of 25; rel SD = 24%), where the minimum was 201 nm and the maximum was 508 nm. As mentioned previously, some needles of HFA-Gal-Cer prepared in 95% 1,2-propanediol or 100% 1,2-ethanediol exceeded 1.5 μm in diameter. There are indications that the dimensions of the needles are affected by such factors as the lipid concentration, solvent composition, degree of mechanical mixing, incubation temperature, and the duration of incubation.

HFA-Gal-Cer Needles Are Cochleate Cylinders. On the basis of their electron density in TEM, the needle structures are seen to be nearly solid. The diameter is often quite constant for a single needle, although there are sometimes narrowed regions, particularly at the ends of a needle. Even when the structures are not completely cylindrical, the structures have rough axial symmetry. There is a small hollow lumen (<7 nm). Moreover, the asymmetric steps near the end are consistent with a "rolled-up sheet" model. The constricted "nodes" in the structure appear to be due to the limited width of an outer wrapping sheet. The lamellar sheet thickness appears to be significantly smaller than two bilayers, indicating that the wrap could be a single bilayer sheet.

In contrast to NFA-Gal-Cer structures, TEM of the HFA-Gal-Cer needles provided no evidence for helical wrapping or helically twisted ribbons. HFA-Gal-Cer needles are also different from diacetylene phospholipid tubules, which often do have a helical substructure, generally have a hollow lumen

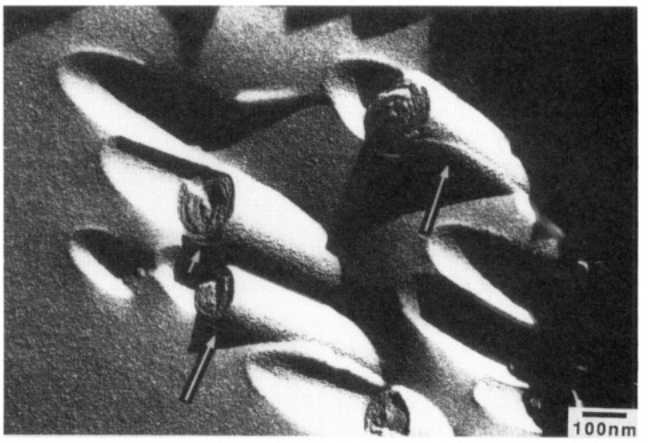

FIGURE 13: Freeze-fracture electron micrograph of HFA-Gal-Cer prepared by thermal/mechanical cycling in 95% 1,2-ethanediol. The arrows points to the edges of lamellae near what are probably broken ends of the needles. Note that this micrograph is printed with dark and light inverted from the usual sense (dark shadows) to improve its readability.

greater than 300 nm, and rarely appear tapered (Yager et al., 1985).

Freeze-fracture electron microscopy shows HFA-Gal-Cer needles to be nearly filled cylinders (see Figure 13). As would be expected for structures composed of rolls of lamellae, the unpaired native edge is sometimes visible on the generally smooth surface. Native edges or ends are those that existed in the suspension before the sample was frozen and fractured. They are differentiable from edges formed by fracturing after freezing, as that type of structure often has irregular edges, and both the convex cylinder and adjacent concavity left by the missing piece are often visible (as in Figure 13). The prevalence of blunt ends may be due to breakage of needles after they form in suspension. The spiral wrapping of the bilayers in these needles identifies them as cochleate lipid cylinders similar to those observed for some negatively charged phospholipids in the presence of high concentrations of Ca^{2+} (Papahadjopoulos et al., 1975; Tocanne et al., 1974; Verkleij et al., 1974; Ververgaert et al., 1975).

Occasionally the outer bilayers of the thickest HFA-Gal-Cer needles fold along the needle axis, converting the outer surface to a series of parallel flat plates (data not shown). A spiralling rippled texture (periodicity on the order of 180 Å) is also occasionally seen on the convex surface of a cylinder or the convacity from removal of a cylinder. These textured replica faces are often found next to smooth replicated structures, indicating that they are not simple artifacts.

By TEM, needles of Gal-Cer in 95% 1,2-ethanediol appear similar to those of HFA-Gal-Cer. However, when a sample of Gal-Cer underwent identical thermal/mechanical history, optical microscopy revealed that the needles of Gal-Cer were shorter and of smaller diameter. Surprisingly, no helical ribbons were observed in Gal-Cer preparations. Moreover, optical microscopy studies indicate that it is possible to obtain complete conversion of Gal-Cer to needles using the procedure described in this paper (data not shown). These observations are supported by calorimetric data that indicated that the HFA-Gal-Cer and NFA-Gal-Cer components of Gal-Cer microstructures in 95% 1,2-ethanediol are not phase separated.

Low-Angle X-ray Scattering of HFA-Gal-Cer Microstructures. Low-angle X-ray scattering of HFA-Gal-Cer needles in 95% 1,2-ethanediol indicated presence of the same predominant 50-Å fundamental repeat distance found in HFA-Gal-Cer granules in 95% 1,2-ethanediol. This approximately

Table II: Characteristics of Cerebroside Microstructures Prepared in 95% 1,2-Ethanediol

	NFA-Gal-Cer	HFA-Gal-Cer
physical form	clear viscoelastic gel	turbid suspension
predominant microstructure	flexible helical fiber	birefringent rigid needle
diameters	85 nm, rel SD ≈ 12%	100–300 nm, rel SD ≈ 25%
lengths	≥10 μm	5–30 μm, rel SD ≥50%, max >300 μm
lumen	≤70 Å	≤70 Å
substructure	rolls of helical ribbons/fibrils	solid rolls of sheets with tapered or blunt ends
surface features	edges of helical wraps, and occasional ≈ 100-Å parallel helical striations	smooth with occasional edges of lamellar wraps, helical striations, and longitudinal facets

corresponds to one of the reported fundamental repeat distances of an anhydrous powdered sample of HFA-Gal-Cer (49 Å) (Fernandez-Bermudez et al., 1977). The measurements on the aqueous suspension indicated that hydrated HFA-Gal-Cer had a predominant fundamental repeat of 65 Å, which corresponds to the other fundamental repeat reported for powdered lipid (Fernandz-Bermudez et al., 1977). The predominant lamellar structure of HFA-Gal-Cer in 95% 1,2-ethanediol is probably fully dehydrated but not interdigitated.

DISCUSSION

Suspension of the cerebrosides in solvents that contain high concentrations of glycols produces changes in the thermal and morphological properties of the lipids. Depending on the specific glycol employed, the phase-transition temperatures of both the complex mixture and its two subfractions are raised by as much as 30 °C, nearing those found for anhydrous materials. In addition, dispersion in glycols is easier than in water, resulting in a gel in the case of NFA-Gal-Cer. Production of high axial ratio microstructures by thermal cycling is changed from a rare occurrence to a quantitative process. The thermal effect of glycols is clearly thermodynamic in origin, but the alteration in morphology could be a result either of changes in thermodynamics or of kinetics of the formation of the microstructures. Table II summarizes various features of the two types of cerebroside microstructures formed in 95% 1,2-ethanediol.

Formation and stabilization of HFA-Gal-Cer needles (cochleate cylinders) seems to involve a complex interplay of molecular and assembly transport, bilayer crystallization, bilayer fusion, and bilayer curvature or adhesion. In our thermal cycling protocol, the formation of the needles can be strongly enhanced by the choice of the suspending solvent. The efficient formation of HFA-Gal-Cer or Gal-Cer needles was not obtained with several other low dielectric constant dehydrating solvents. 1,2-Propanediol was partially effective on HFA-Gal-Cer but appeared ineffective for Gal-Cer cylinder formation. Relatively or completely ineffective solvents included ethanol or glycerol, which are molecularly similar to 1,2-ethanediol and/or have similar bulk physical properties. Processing conditions can cause considerable variation in the lipid microstructure produced. Compared to NFA-Gal-Cer, the expression of various microstructural morphologies of HFA-Gal-Cer is even more sensitive to the conditions of preparation. Indeed, the most stable phase may be infinite sheets of stacked bilayers composed of ideal mixtures of the molecular components, while needles and related structures may simply be kinetically trapped products of slightly higher energy.

The existence of a multiplicity of phases, some of which are metastable, has been known for some time for both Gal-Cer (Bunow, 1979) and glucocerebrosides (Freire et al., 1980). Even dry NFA-Gal-Cer has at least four different phases (Hosemann et al., 1979). Previous work by Curatolo (1985) reported that addition of 1,2-ethanediol eliminates the metastable thermal behavior of C16:0-Cer, a form of NFA-Gal-Cer. He attributed the solvent's effect to dehydration of the headgroup such that the system was not able to form a metastable hydrated state. In 50% 1,2-ethanediol or DMSO, he observed a 10 °C decrease in the temperature of the gel-to-liquid-crystalline heating endotherm, which also had a smaller enthalpy than in water. In sharp contrast to the results of Curatolo, at higher concentrations, 90–95% 1,2-ethanediol or 1,2-propanediol, we observe a large increase in T_m.

Glycols such as 1,2-ethanediol and other cryoprotectants have been shown to induce new phases in other glycolipids, such as galactosyldiacylglycerols (Sen et al., 1982). In aqueous suspension, it has been shown that glucocerebroside (the glucose analog of NFA-Gal-Cer) has four unfreezable water molecules per lipid molecule (Bach et al., 1982). Part or all of this water may either be displaced or simply extracted by 1,2-ethanediol, resulting in altered headgroup hydrogen bonding. This may account for the more thermally stable gel phase in 1,2-ethanediol. This study indicates that this putative dehydration assists in the formation of a stable helical ribbon gel form of NFA-Gal-Cer.

The divergent efficiencies of the different glycols implicate a specific interaction between glycol and cerebroside. 1,2-Propanediol and 1,2-ethanediol are similar in most physical properties, yet the same mole fraction of the smaller molecule is about twice as effective in shifting T_m (see Table I). If the primary role of the glycols were simply reduction of the activity of water molecules, 1,2-ethanediol would be expected to be no more than 20% more effective because of its higher number concentration. There is a fundamental difference between the solvents that may easily account for the difference in effectiveness: 1,2-ethanediol is a single achiral molecular species, whereas the 1,2-propanediol used was a 1:1 (racemic) mixture of enantiomers. If a specific spatial orientation of the two vicinal hydroxyl groups is required for proper hydrogen bonding to the lipid headgroup in the "dehydrated" form, and if steric hindrance blocks the presence of a bulky substituent for one of the hydrogens on the middle carbon of 1,2-propanediol, then only one of its enantiomers will fit into the binding site. An example of such a set of conformations for the glycols is shown in Figure 14. The concentration of the *effective* isomer in 95% racemic 1,2-propanediol would then be *exactly half* that in the case of 95% 1,2-ethanediol.

On the basis of the TEM images, 1,2-ethanediol does not appear to alter the type of structures that can form from NFA-Gal-Cer. The solvent only seems to increase the number of bilayer wraps and increase the tightness of packing. In addition, NFA-Gal-Cer forms a gel in a variety of nonaqueous solvents, and fast cooling rates do not inhibit gel formation. Helical NFA-Gal-Cer structures can form in water, but dispersion is poor and most of the lipid tends to form vesicles while much remains condensed and in no recognizable microstructure. NFA-Gal-Cer gels can also be quantitatively

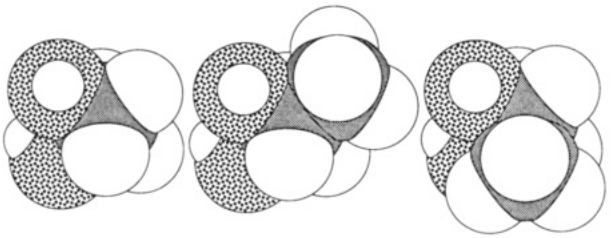

FIGURE 14: Molecular models of a minimized structure for 1,2-ethanediol (left) and models of both the *R* and *S* isomers of 1,2-propanediol built on the first structure and viewed along the C–C axis of 1,2-ethanediol. The additional methyl group in 1,2-propanediol molecule is placed on the upper carbon. Steric interactions with a putative glycol binding site could exclude one 1,2-propanediol isomer relative to the other.

formed without thermal cycling by simple water precipitation from pyridine solution, suggesting that the helical or twisted ribbon is the thermodynamically most stable form of the NFA-Gal-Cer fraction, as for diacetylenic lipids (Chappell & Yager, 1991b,c; Georger et al., 1987). HFA-Gal-Cer and Gal-Cer are even more difficult to disperse in water and appear to remain almost completely granular or vesicular. Helices are absent, though a few extended lamellar sheets appear to form elongated structures. The presence of the HFA-Gal-Cer fraction of Gal-Cer disrupts extensive formation of the helical microstructures that are found in pure NFA-Gal-Cer.

The occasional spiraling striated texture observed on the surface of lamellar wraps in both NFA-Gal-Cer and HFA-Gal-Cer may be related to the structure seen on the surface of glucosylceramide deposits in Gaucher's disease (Lee, 1968; Naito et al., 1988) that have superficial appearance of an inverted hexagonal (H_{II}) phase. The H_{II} phase is known to occur in monogalactosyldiglyceride, another two-chain amphiphile containing a single sugar residue in the headgroup (Curatolo, 1987; Lindblom & Rilfors, 1989). While these lipids are cycled to extremely high temperatures at which they might assume a H_{II} phase, the equilibrium phase of the lipids is crystalline at temperatures at which they were observed in this study. If the striations do reflect an underlying H_{II} phase, it is a minor metastable form that has been kinetically trapped (supercooled) by the thermal cycling.

One surprising result of these studies is that it is possible to produce high axial ratio microstructures quantitatively from the relatively crude biological extract containing a mixture of fatty acyl chains. This implies that packing of the headgroups (which extends down to the hydroxyl groups in HFA-Gal-Cer) controls formation of this helical lipid microstructure. The chain heterogeneity may account for the irregularity in NFA-Gal-Cer microstructures that contrasts with the reports of amino acid containing ammonium amphiphiles (Nakashima et al., 1984; Yamada et al., 1984) and the diacetylene phospholipids (Yager & Schoen, 1984), both of which form straight regular helices and/or tubules. Gal-Cer, the native mixture of HFA-Gal-Cer and NFA-Gal-Cer, forms needle-like cochleate cylinders by thermal cycling in 95% 1,2-ethanediol. Since complete phase separation does not occur, in Gal-Cer the 45% HFA-Gal-Cer present imposes its crystal packing on the structure of the crystallizing mixture.

Studies by Pascher (1976) indicate that the amide group of sphingolipids such as ceramide "control" the molecular conformation in crystal forms via hydrogen-bonding interactions. Pascher and Sundell (1977) have published a crystal structure of β-D-galactosyl-*N*-(2-D-hydroxyoctadecanoyl)-D-dihydrosphingosine, a minor component of HFA-Gal-Cer lacking the typical unsaturation in the sphingosine backbone and having an atypically short α-hydroxyacyl chain. The α-hydroxy group of the acyl chain, the amide N–H, and the glycoside oxygen are involved in important hydrogen bonds that effectively distort the hydrocarbon chain packing and pull the sugar ring toward the hydrocarbon region. The molecule is probably a good model for dehydrated HFA-Gal-Cer headgroup interactions because calorimetric studies show that headgroup interactions typically dominate chain length effects in cerebrosides (Maggio et al., 1985) and because a similar diffraction pattern was observed for the analog having the usual unsaturated sphingosine (Pascher & Sundell, 1977). X-ray scattering of HFA-Gal-Cer indicates a large degree of chain tile in the gel phase (Fernandez-Bermudez et al., 1977) that is lost on melting, and the lamellar spacing of dry HFA-Gal-Cer increases from approximately 50 Å in the crystalline phases to approximately 80 Å in the first liquid-crystalline phase (Agrahamsson et al., 1972). This may explain the volume increase and lack of morphological reversibility observed when HFA-Gal-Cer needles are melted. Surprisingly, Pascher and Sundell (1977) found that there is no interbilayer hydrogen bonding and the few interbilayer ethanol molecules are not arranged in a regular array. In this dehydrated crystal, nearly all the possible hydrogen-bond donor and acceptor sites are occupied. The only two acceptor sites remaining are the oxygen in the galactose ring and the oxygen forming the glycoside linkage. Because of extensive intrabilayer hydrogen binding, HFA-Gal-Cer apparently has the capacity to form stable and separate dehydrated bilayers.

Because of the absence of α-hydroxy groups, the conformation of NFA-Gal-Cer in pure bilayers is probably quite different from that seen with purified and dehydrated HFA-Gal-Cer bilayers. This is supported by Raman data on the two lipid systems (Bunow & Levin, 1980). We attribute difference in microstructures to be primarily due to the addition of the α-hydroxy groups. The differences between the Gal-Cer subfractions in the degree of saturation and chain length of the fatty acyl chains probably play only a secondary role in microstructure formation.

Recent surface force measurements (Israelachvili & McGuiggan, 1988) with dialkylphosphatidylglycerol [which forms cochleate cylinders in the presence of Ca^{2+} (Tocanne et al., 1974)] have shown that in the presence of Ca^{2+} there is essentially no repulsive hydration force (Marra, 1986). Consequently, strong forces pull the bilayer surfaces into direct contact once double layer repulsion is overcome. Surface force studies have also been carried out on the neutral lipid monogalactosyldiglyceride (Marra, 1985) that has a molecular structure crudely similar to HFA-Gal-Cer. In water, this lipid has an attractive van der Waals force at long distances, but this is offset by a hydration force. The combination of forces results in an adhesion energy minimum at 6 Å out from the estimated anhydrous layer boundary. The reported structure of HFA-Gal-Cer is characterized by a triclinic unit cell with chains partially interdigitated and tilted at 45° from the normal to the bilayer. The wide-angle scattering revealed that this structure has nearly the same lattice cell as the paraffin $C_{20}H_{42}$ (Fernandez-Bermudez et al., 1977). This implies very tight packing of the hydrocarbon chains and is consistent with the apparent rigidity and brittleness of the needles.

The X-ray scattering data of this work indicates that HFA-Gal-Cer bilayers in 95% 1,2-ethanediol are brought into close if not direct steric contact such as is observed in the completely dehydrated lipid. Ethylene glycol and other nonaqueous solvents have been shown to promote membrane fusion in some lipid systems (Simon & McIntosh, 1984). This is an

important observation because close membrane contact through adhesion is thought to be a necessary precursor to membrane fusion (Ahkong et al., 1975). Moreover, membrane fusion is almost certainly involved in the growth of HFA-Gal-Cer needles. In aqueous suspension, cerebroside bilayers have about eight or nine unfreezable water molecules per lipid molecule (Bach et al., 1982). Glucocerebroside, the glucose analog of NFA-Gal-Cer, has only four. Therefore HFA-Gal-Cer may have more than four unfreezable water molecules per lipid, some or all of which may be eliminated either by displacement or simple reduction in activity by suspension of the lipids in high concentrations of 1,2-ethanediol.

Biological Relevance of Cerebroside Microstructures. There are many examples of high axial ratio lipid structures in nature, and in some of these cases self-assembly of the lipids may at least partially contribute to their stability. For example, there are high axial ratio lipid microstructures in deposits found in globoid-cell leukodystrophy (GLD, galactosylceramide lipidosis, or Krabbe's disease) (Suzuki & Suzuki, 1989). GLD is a rare fatal disease caused by a genetic deficiency of galactocerebroside β-galactosidase (also known as galactosylceramidase) characterized by the appearance of globoid cells in brain white matter and the degradation of oligodendrocytes and myelin. Gal-Cer accumulates inside the globoid cells. The deposits themselves are highly anisotropic and fall into two classes as observed by electron microscopy; one is a straight or gently arched tubular deposit that in cross-section appears angular (Andrews & Cancilla, 1970; Blinzinger & Anzil, 1971; Schochet et al., 1969; Suzuki, 1970). The second class is made up of smaller diameter tubules twisted in a right-handed helix with a rectangular or irregularly round cross-section (Suzuki, 1970; Yunis & Lee, 1969, 1970). The small tubule diameter was measured to be 23–35 nm while the helical pitch was typically 150–300 nm. Both inclusion types frequently have periodic longitudinal bands (circa 60 Å). How these deposits form is unknown.

The relative amount of the two types of GLD inclusions varies with the sample preparation and the particular patient. Globoid cells can also be produced experimentally by the injection of Gal-Cer into normal brain tissue (Suzuki, 1970). Usually this procedure results primarily in the only the larger crystalloid structure (Andrews & Menkes, 1970). It has also been noted that the two types of inclusions are morphologically similar to some seen in samples of negatively stained pure brain Gal-Cer (Suzuki, 1970; Yunis & Lee, 1969, 1970). Thus it appears that the morphology of Gal-Cer deposits in GLD is largely controlled by the lipid itself. Some reports of composition of globoid cell deposits indicate enrichment in NFA-Gal-Cer (Pilz, 1964; Suzuki & Suzuki, 1989), which could explain why the helical structure is observed.

A related lipid storage disease, Gaucher's disease, is characterized by lipid deposits in modified macrophages; these deposits are very stable stacks of six to 12 bilayers that form twisted ribbons (Lee, 1968; Lee et al., 1973; Naito et al., 1988) very similar to those produced by pure NFA-Gal-Cer. This is consistent because the Gaucher's deposits are composed of glucosylceramide that does has no α-hydroxylacyl moieties (Curatolo, 1987).

Lipid self-assembly might also have a hand in movement of biological membranes. The process of helix or tubule formation involves a great deal of membrane movement that could be used for membrane transport in a biological system. Myelin formation by Schwann cells may be facilitated by the tendency of the lipids involved to roll up into cochleate cylinders.

SUMMARY

This work strengthens the relevance of high axial ratio lipid microstructures to normal biological function. The lipid inclusions found in lipid storage diseases are almost certainly the same crystalline or polycrystalline forms generated by thermal cycling in solvents. NFA-Gal-Cer microstructures are bilayers that spontaneously arrange themselves as helical ribbons or helically wrapped tubules similar to those produced by a number of synthetic amphiphiles. The microstructures were produced quantitatively by thermal/mechanical cycling in aqueous miscible solvents or by room temperature precipitation from pyridine–water solution. These NFA-Gal-Cer microstructures appear similar to those characteristic of lipid deposits in the disease GLD. HFA-Gal-Cer or Gal-Cer do not readily form the types of microstructures that are considered characteristic of GLD but may be responsible for the granular and crystalloid deposit forms.

The formation of cochleate cylinders from Gal-Cer is particularly suggestive because the lipid comprises a significant fraction of myelin. Moreover, the fact that it is the HFA-Gal-Cer fraction that forms cochleate needles is significant because α-hydroxy fatty acids are rare in non-myelin tissues. Myelin consists of several proteins and lipids so such a role of lipids in stabilization has not been proven. However, because the form of HFA-Gal-Cer and Gal-Cer microstructures is myelin-like, the lipid interactions alone may help stabilize a myelin structure, as previously suggested (Curatolo & Neuringer, 1986). Of course the route to formation of helical microstructures in vivo involves neither high concentrations of 1,2-ethanediol nor cycling to 90 °C. Other carbohydrates may substitute for low molecular weight glycols, or it may be that the metabolic production of the lipids acts as a source for slow accretion of the cerebrosides onto the microstructures in a method analogous to solvent precipitation from pyridine.

The fact that different microstructures form from HFA-Gal-Cer and NFA-Gal-Cer despite the similarity in their molecular structures reinforces the pivotal role of molecular crystal packing in lipid microstructure formation. Cochleate needles appear to be a "default" structure for bilayers with extremely strong headgroup attraction (*inter*bilayer packing) independent of the quality of the hydrocarbon chain packing. Helical and hollow tubule-type structures form in response to strong anisotropic long-range *intra*bilayer packing interactions that appear to go hand-in-hand with tight hydrocarbon chain packing. When both intra- and interbilayer forces are strong, one develops stacked helical structures such as those seen in NFA-Gal-Cer.

ACKNOWLEDGMENT

We thank Dr. Marie Cantino for her expertise and assistance with transmission and freeze-fracture electron microscopy and Leslie Sack for assistance with final production of the manuscript.

REFERENCES

Abrahamsson, S., Pascher, I., Larsson, K., & Karlsson, K. A. (1972) *Chem. Phys. Lipids 8*, 152–179.

Ahkong, Q. F., Fisher, D., Tampion, W., & Lucy, J. A. (1975) *Nature 253*, 194–195.

Andrews, J. M., & Cancilla, P. A. (1970) *Arch. Pathol. 89*, 53–55.

Andrews, J. M., & Menkes, J. H. (1970) *Exp. Neurol. 29*, 483–493.
Archibald, D. D. (1990) *Structural Studies of High Aspect-Ratio Self-Assembled Lipid Microstructures with the Use of Microscopy and FT–NIR–Raman Spectroscopy*, Ph.D. Dissertation, University of Washington.
Bach, D., Sela, B., & Miller, I. R. (1982) *Chem. Phys. Lipids 31*, 381–394.
Blechner, S. L., Skita, V., & Rhodes, D. G. (1990) *Biochim. Biophys. Acta 1022*, 291–295.
Blinzinger, K., & Anzil, A. P. (1971) *Experientia 28*, 780–781.
Bunow, M. R. (1979) *Biochim. Biophys. Acta 574*, 542–546.
Bunow, M. R., & Levin, I. W. (1980) *Biophys. J. 32*, 1007–1021.
Burke, T. G., Rudolph, A. S., Price, R. R., Sheridan, J. P., Dalziel, A. W., Singh, A., & Schoen, P. E. (1988) *Chem. Phys. Lipids 48*, 215–30.
Chappell, J. S., & Yager, P. (1991a) *Biophys. J. 60*, 1–14.
Chappell, J. S., & Yager, P. (1991b) *Chem. Phys. 150*, 73–79.
Chappell, J. S., & Yager, P. (1991c) *Chem. Phys. Lipids 58*, 253–258.
Curatolo, W. (1982) *Biochemistry 21*, 1761–1764.
Curatolo, W. (1985) *Biochim. Biophys. Acta 817*, 134–138.
Curatolo, W. (1987) *Biochim. Biophys. Acta 906*, 111–136.
Curatolo, W., & Jungalwala, F. B. (1985) *Biochemistry 24*, 6608–6613.
Curatolo, W., & Neuringer, L. J. (1986) *J. Biol. Chem. 261*, 17177–17182.
de Gennes, P.-G. (1987) *C. R. Acad. Sci., Ser. 3 304*, 259–263.
Fernandez-Bermudez, S., Loboda-Cackovic, J., Cackovic, H., & Hosemann, R. (1977) *Z. Naturforsch. 32*, 362–372.
Freire, E., Correa-Freire, M., Miller, I., & Barenholz, Y. (1980) *Biochemistry 19*, 3663–3665.
Fuhrhop, J. H., Schnieder, P., Rosenberg, J., & Boekema, E. (1987) *J. Am. Chem. Soc. 109*, 3387–3390.
Fuhrhop, J. H., Schnieder, P., Boekema, E., & Helfrich, W. (1988) *J. Am. Chem. Soc. 110*, 2861–2867.
Georger, J., Price, R., Singh, A., Schnur, J. M., Schoen, P. E., & Yager, P. (1987) *J. Am. Chem. Soc. 109*, 6169–6175.
Helfrich, W. (1986) *J. Chem. Phys. 85*, 1085–1087.
Helfrich, W., & Prost, J. (1988) *Phys. Rev. A 38*, 3065–3068.
Hosemann, R., Loboda-Cackovic, J., Cackovic, H., Fernandez-Bermudez, S., & Balta-Calleja, F. J. (1979) *Z. Naturforsch. 34*, 1121–1124.
Israelachvili, J., & McGuiggan, P. M. (1988) *Science 241*, 795–800.
Johnston, D., & Chapman, D. (1988) *Biochim. Biophys. Acta 937*, 10–22.
Lee, R. E. (1968) *Pathology 61*, 484–489.
Lee, R. E., Worthington, C. R., & Glew, R. H. (1973) *Arch. Biochem. Biophys. 159*, 259–266.
Lindblom, G., & Rilfors, L. (1989) *Biochim. Biophys. Acta 988*, 221–256.
Maggio, B., Ariga, T., Sturtevant, J. M., & Yu, R. K. (1985) *Biochim. Biophys. Acta 818*, 1–12.
Marra, J., (1985) *J. Colloid Interface Sci. 107*, 446–458.
Marra, J. (1986) *Biophys. J. 50*, 815–825.
McCabe, P. J., & Green, C. (1977) *Chem. Phys. Lipids 20*, 319–330.
Naito, M., Takahashi, K., & Hojo, H. (1988) *Lab. Invest. 58*, 509–598.
Nakashima, N., Asakuma, S., Kim, J. M., & Kunitake, T. (1984) *Chem. Lett.*, 1709–1712.
Nakashima, N., Asakuma, S., & Kunitake, T. (1985) *J. Am. Chem. Soc. 107*, 510–512.
Papahadjopoulos, D., Vail, W. J., Jacobson, K., & Poste, G. (1975) *Biochim. Biophys. Acta 394*, 483–491.
Pascher, I. (1976) *Biochim. Biophys. Acta 455*, 433–451.
Pascher, I., & Sundell, S. (1977) *Chem. Phys. Lipids 20*, 175–191.
Pilz, H. (1964) *Acta Neuropathol. 4*, 16–27.
Rhodes, D. G., Blechner, S., Schoen, P. E., & Yager, P. (1987) *Biophys. J. 51*, 527.
Rhodes, D. G., Blechner, S. L., Yager, P., & Schoen, P. E. (1988) *Chem. Phys. Lipids 49*, 39–47.
Rudolph, A. S., Calvert, J. M., Schoen, P. E., & Schnur, J. M. (1988) in *Biotechnological Applications of Lipid Microstructures* (Gaber, B. P., Schnur, J. M., & Chapman, D., Eds.) pp 305–320, Plenum Publishing Corp., New York.
Schnur, J. M., Price, R., Schoen, P., Yager, P., Calvert, M., Georger, J., & Singh, A. (1987) *Thin Solid Films 152*, 181–206.
Schochet, S. S. J., Hardman, J. M., Lampert, P. W., & Earle, K. M. (1969) *Arch. Pathol. 88*, 305 313.
Sen, A., Brain, A. P. R., Quinn, P. J., & Williams, W. P. (1982) *Biochim. Biophys. Acta 686*, 215–224.
Servuss, R. M. (1988) *Chem. Phys. Lipids 46*, 37–41.
Simon, S. A., & McIntosh, T. J. (1984) *Biochim. Biophys. Acta 773*, 169–172.
Suzuki, K. (1970) *Lab. Invest. 23*, 612–619.
Suzuki, K. & Suzuki, Y. (1989) in *The Metabolic Basis of Inherited Disease II* (Scriver, C. M., Ed.) 6th ed., pp 1699–1720, McGraw-Hill, San Francisco, CA.
Tocanne, J. F., Ververgaert, P. H. J. T., Verkleij, A. J., & van Deenen, L. L. M. (1974) *Chem. Phys. Lipids 12*, 201–219.
Verkleij, A. J., de Kruyff, B., Ververgaert, P. H. J. T., Tocanne, J. F., & van Deenen, L. L. M. (1974) *Biochim. Biophys. Acta 339*, 432–437.
Ververgaert, P. H. J. T., de Kruyff, B., Verkleij, A. J., Tocanne, J. F., & van Deenen, L. L. M. (1975) *Chem. Phys. Lipids 14*, 97–101.
Yager, P., & Schoen, P. E. (1984) *Mol. Cryst. Liq. Cryst. 106*, 371–381.
Yager, P., Schoen, P. E., Davies, C., Price, R. R., & Singh, A. (1985) *Biophys. J. 48*, 899–906.
Yager, P., Price, R. R., Schnur, J. M., Schoen, P. E., Singh, A., & Rhodes, D. G. (1988) *Chem. Phys. Lipids 46*, 171–179.
Yager, P., Chappell, J., & Archibald, D. D. (1992) in *Biomembrane Structure & Function: The State of the Art* (Gaber, B. P., & Easwaran, K. R. K., Eds.) pp 1–19, Adenine Press, Schenectady, NY.
Yamada, K., Ihara, H., Ide, T., Fukumoto, T., & Hirayama, C. (1984) *Chem. Lett.* 1713–1716.
Yunis, E. J., & Lee, R. E. (1969) *Lab. Invest. 21*, 415–419.
Yunis, E. J., & Lee, R. E. (1970) *Science 169*, 64–66.